Methanol Synthesis from CO_2 Hydrogenation with a Cu/Zn/Al/Zr Fibrous Catalyst[*]

AN Xin (安欣)**, ZUO Yizan** (左宜赞)**, ZHANG Qiang** (张强) **and WANG Jinfu** (王金福)[**]
Beijing Key Laboratory of Green Chemical Reaction Engineering and Technology, Department of Chemical Engineering, Tsinghua University, Beijing 100084, China

Abstract   A highly active Cu/Zn/Al/Zr fibrous catalyst was developed for methanol synthesis from CO_2 hydrogenation. Various factors that affect the activity of the catalyst, including the reaction temperature, pressure and space velocity, were investigated. The kinetic parameters in Graaf's kinetic model for methanol synthesis were obtained. A quasi-stable economical process for CO_2 hydrogenation through CO circulation was simulated and higher methanol yield was obtained.
Keywords   kinetics, CO_2 hydrogenation, methanol, Cu/Zn/Al/Zr catalyst

1   INTRODUCTION

The greenhouse effect is a threat to the living environment of mankind. The transformation of CO_2 into useful chemicals, *e.g.* methanol, is an attractive way to protect the global environment since CO_2 is an important greenhouse gas and methanol itself is a useful raw chemical and solvent [1, 2]. For methanol synthesis, Cu/Zn based catalysts were always used [3-16]. Various catalysts, including Cu/Zn/Al, Cu/Zn/Cr, Cu/Zn/Zr, Cu/Zn/Ga, Cu/Zn/Ge *et al*. [7-11, 14, 15], were developed for methanol synthesis. It is believed that Cu adsorbs CO_2 and Zn adsorbs H_2, and the reaction takes place on the surface of the catalyst. Thus, a catalyst with good Cu/Zn dispersion is a key factor for high yield and selectivity for methanol synthesis. Among many catalysts, the Cu/Zn/Al catalyst has been commonly used in various studies, and a lot of modified Cu/Zn/Al based catalysts were reported recently [8, 11, 15, 17]. Using the phase separation effect of nanoparticles on a catalyst surface, a fibrous Cu/Zn/Al/Zr catalyst that is active for methanol production from CO_2 hydrogenation was prepared by our group recently [16]. A 5% Zr addition led to a methanol space time yield 80% higher than that on the commercial catalyst that is the present catalyst of choice in China.

However, for CO_2 hydrogenation, there is a competing process between the reverse water shift reaction and methanol synthesis reaction. The reverse water shift reaction reaches thermodynamic equilibrium fast, while the methanol synthesis reaction is much slower. Although the catalyst showed a high activity and high methanol yield, CO, which was the product of the reverse water shift reaction, was present in the final product. From the viewpoint of the utility of the carbon source, no CO should be produced during methanol synthesis process because CO can be

recycled into the reactor for methanol synthesis. To understand the concept further, the first step is to understand the catalytic behavior and develop the kinetic model. There have been some kinetic studies of methanol synthesis from CO_2 hydrogenation. The catalysts were Cu/Zn/Al, Pt-Ca/C, or Cu/Zr based, which showed lower activity than the novel fibrous Cu/Zn/Al/Zr catalyst [3-6, 13, 17]. Kinetics data for the Cu/Zn/Al/Zr catalyst on CO_2 hydrogenation to methanol had not been reported, and the kinetic model was developed in this work as a basis for us to understand the catalytic behavior and design a process of CO_2 hydrogenation.

In this work, the fibrous Cu/Zn/Al/Zr catalyst was used in CO_2 hydrogenation to methanol at various temperature, pressure and space velocity. Base on the regression parameters fitted to the assumed Graaf's kinetic model, a CO_2 hydrogenation process that CO cycle in the system was simulated, the space time yield of methanol increased, which was helpful for scaling up this process in future.

2   EXPERIMENTAL

The fibrous Cu/Zn/Al/Zr catalyst was prepared by a novel co-precipitation procedure reported recently [17]. Typically, the solution of $Cu(NO_3)_2 \cdot 6H_2O$, $Zn(NO_3)_2 \cdot 6H_2O$, $Al(NO_3)_3 \cdot 6H_2O$ and $ZrOCl_2$ with a concentration of $0.6 \ mol \cdot L^{-1}$ were mixed with a ratio of 6 : 3 : 0.5 : 0.5, then the mixture was precipitated with the solution Na_2CO_3 at 353 K with strong stirring for 1 h. After filtration and washing, the catalyst was dried at 120°C for 12 h and calcined at 350°C for 4 h to give the Cu/Zn/Al/Zr catalyst. The prepared catalyst was ground into powder and mixed with SiO_2, and load into the fixed bed reactor.

The catalytic reaction on the Cu/Zn/Al/Zr catalyst was carried out in a fixed bed reactor. The reactor

---

is with a diameter of 12 mm and a length of 500 mm. The catalyst is packed at the middle section (about 100 mm) of the reactor, where the temperature was uniform. All of the gas, including the hydrogen, nitrogen, and carbon dioxide, is of purity above 99.999%. Thus, other impurity in industrial, such as CO, H_2S, COS, was neglected. Before reaction, the catalyst was reduced with a 5% H_2/95% N_2 mixture at atmospheric pressure by raising the temperature slowly to the reaction temperature over 10 h. Then the reduction gas was switched to the reaction gas and the pressure was raised to the reaction pressure to start the reaction. The first sample of the effluent was taken 2 h after steady reaction conditions were established, and then samples were taken every 30 min for online analysis of the effluent composition. The reaction temperature was controlled by furnace heating and the pressure was controlled by the feeding rate.

The structure of the catalysts was studied by using Transmission Electron Microscope (TEM) and N_2 adsorption method. The morphology of the Cu/Zn/Al/Zr catalyst was characterized by a JEM 2010 high resolution scanning electron microscope (SEM) operated at 120.0 kV. The BET surface area was obtained with a high resolution BET equipment described in Li *et al* [18].

The reaction equipment is connected on-line to a GC 7890II gas chromatograph provided with a thermal conductivity detector (TCD), a Porapak T (5 m) column parallel connected with a TDX-01 (3 m) column. All detector and columns are placed in the oven and operate within the 0−150°C range. A Porapak T column was used for separation of MeOH and H_2O, and a TDX-01 column was used for separation of H_2, CO, and CO_2. CO_2 conversion, MeOH yield and CO yield are defined as follows:

$$X_{CO_2} = \frac{n_{CO_{2,in}} - n_{CO_{2,out}}}{n_{CO_{2,in}}} \qquad (1)$$

$$Y_{MeOH} = \frac{n_{CH_3OH,out}}{n_{CO_{2,in}}} \qquad (2)$$

$$Y_{CO} = \frac{n_{CO,out}}{n_{CO_{2,in}}} \qquad (3)$$

where n_{CO} and n_{CO_2} are the molar flow rates of CO, and CO_2, respectively. Subscripts "in" and "out" denote represent the inlet and outlet.

Space time yield of MeOH, S_{MeOH}, which describes the amount of MeOH, CO production on per gram catalyst per second, is defined and calculated using the following equation:

$$S_{MeOH} = Y_{MeOH} \times V_{CO_2} \times M_{MeOH} \times 0.001$$
$$(kg \cdot g^{-1})/22.4 \ (L \cdot mol^{-1}) \qquad (4)$$

where Y_{MeOH} is the yield of MeOH, V_{CO_2} the space velocity of CO_2, and M_{MeOH} the molecular weight of MeOH.

3 METHANOL SYNTHESIS FROM CO_2 HYDROGENATION

A fibrous Cu/Zn/Al/Zr catalyst (12∶6∶1∶1) was used to catalyze methanol synthesis in the fixed bed. As shown in Fig. 1, the Cu/Zn/Al/Zr catalyst existed as regular one-dimensional nanomaterial agglomerates. In the fibrous Cu/Zn/Al/Zr catalyst, the effect of Zr incorporation on the metallic function used for methanol synthesis were two aspects, the first is the phase separation effect [16, 19], which was attributed from fibrous agglomerate morphology and the slow rate for Cu/Zn sintering, The second factor for the high activity of a Cu/Zn/Al/Zr catalyst is related to the effect of ion doping and valence compensation. Zr^{4+} dissolved in the ZnO crystal causes the formation of positive ion defects on the surface of Cu-ZnO. These defects can adsorb Cu^+ and form and stabilize more active sites, Cu^0-Cu^+-O-Zn^{2+}, on the catalyst surface [16]. Thus, a high performance of methanol catalyst that with a BET surface area of 70.9 $m^2 \cdot g^{-1}$ was obtained. This was used in the CO_2 hydrogenation.
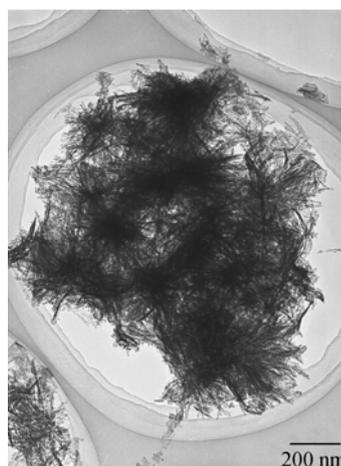
Figure 1   TEM images of the fibrous catalyst

If the space velocity was above 900 ml·(g cat)$^{-1} \cdot h^{-1}$ in the present reactor, the external diffusion was not shown. Furthermore, the size of the catalyst particles should be less than 0.35 mm to avoid internal diffusion, which similar to previous reports [20−23]. In the present studies, the space velocities in the kinetic experiments were all above 1000 ml·(g cat)$^{-1} \cdot h^{-1}$, and the particle size of the Cu/Zn/Al/Zr catalyst was less than 0.05 mm. The thermodynamics of methanol synthesis reactions were also studied similar to the previous reports [24]. The equilibrium constants at different temperatures were calculated using van Hoff equation as below:

$$\left(\frac{\partial \ln K_f}{\partial T} \right)_p = \frac{\Delta H_R^0}{RT^2} \qquad (5)$$

These were used to calculate the equilibrium conversions and yields for given initial conditions. In the

following parts, various factors, including reaction temperature, pressure, and space velocity have a large effect on methanol synthesis.

3.1   The effect of reaction temperature

CO_2 hydrogenation takes place at temperatures from 483 to 543 K. The relationship between reaction temperature and CO_2 conversion or methanol yield is shown in Fig. 2. Methanol synthesis and the reverse water shift reaction occurred in the reactor. When the reaction temperature was higher, the reaction rate increased, and more CO_2 was converted into methanol when the system is far from thermodynamic equilibrium. At 523 K, CO_2 conversion can reach 0.258. However, the CO_2 conversion was decreased to 0.251 when the temperature was 543 K because of thermodynamic equilibrium. With the increase of temperature, the CO_2 conversion reached to thermodynamic gradually. Moreover, methanol yield, which is the lower line in Fig. 2, showed trends similar to CO_2 conversion. It was noticed that only a fraction of CO_2 was converted to methanol, while the rest was converted to CO. Methanol yield increased from 11.4% at 483 K to 17.9% at 523 K, which is 36% higher than the yield at 483 K. However, although methanol synthesis is an exothermic process and the temperature increasing further is not favorable, but because the reverse water shift reaction is endothermic, which resulted in that the methanol yield was decreased. We can also see that methanol synthesis was more sensitive than the reverse water shift reaction with respect to the reaction temperature. The fibrous catalyst has its highest methanol yield at 523 K at a space velocity of 6000 ml·(g cat)$^{-1}$·h^{-1} and a pressure of 5 MPa.
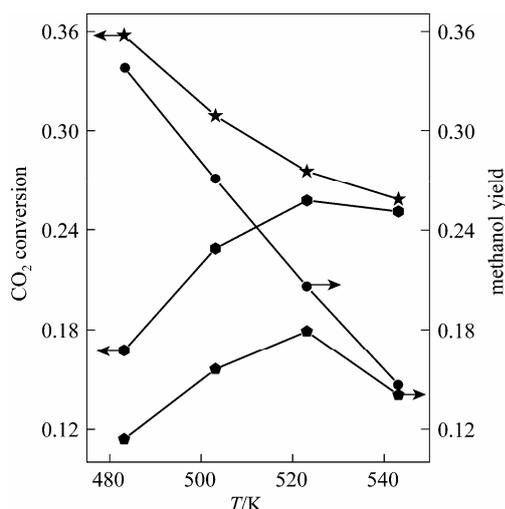
Figure 2   Relationship between the reaction temperature and CO_2 conversion and methanol yield from the experimental (exp.) **results and thermodynamic** (ther.) **predictions** [y_{H_2} : y_{CO_2} = 3 : 1, p = 5 MPa, SV = 6000 ml·(g cat)$^{-1}$·h^{-1}]
● conversion, exp.; ★ conversion, ther.; ♠ yield, exp.;
● yield, ther.

3.2   The effect of pressure

From the thermodynamics, a high pressure is beneficial for methanol production from CO_2. On the fibrous Cu/Zn/Al/Zr catalyst, the relationship between the pressure and CO_2 conversion and methanol yield is shown in Fig. 3. At 2.0 MPa, CO_2 conversion was just 0.190. When the pressure was increased to 5.0 MPa, CO_2 conversion was increased to 0.258. When the pressure increased, the difference between the experimental results and thermodynamic equilibrium was also increased. Furthermore, the yield of methanol also showed similar trends: methanol yield was 0.061 and 0.179 at pressures of 2.0 and 5.0 MPa, respectively. It was also observed that the methanol yield increased faster than the CO_2 conversion which meant that methanol synthesis was more sensitive than the reverse water shift reaction with respect to the reaction pressure. This is in agreement with many other reports. A high pressure was also effective for the Cu/Zn/Al/Zr catalyst in our case. Meanwhile, the flow rate through the reactor was also increased. Too high a reaction pressure has a much higher requirement for the material of the facility and also poses a safety problem.
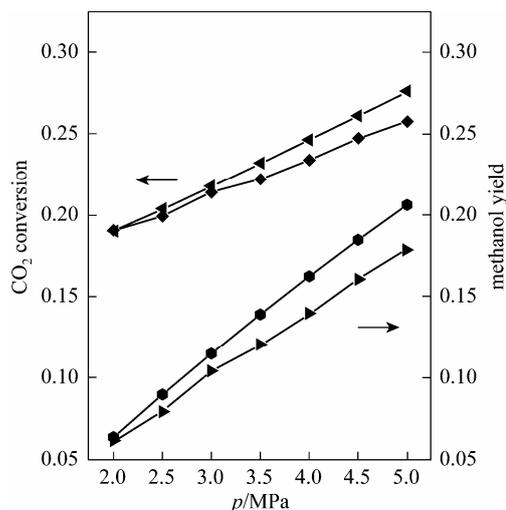
Figure 3   Relationship between the pressure and CO_2 conversion and methanol yield from the experimental (exp.) **results and thermodynamic** (ther.) **predictions** [SV = 6000 ml·(g cat)$^{-1}$·h^{-1}, y_{H_2} : y_{CO_2} = 3 : 1, T = 523 K]
◆ conversion, exp.; ◄ conversion, ther.; ► yield, exp.;
● yield, ther.

3.3   The effect of the space velocity

The space velocity, which is a parameter that reflects the reactor efficiency, was also tested with a H_2/CO_2 ratio of 3 and a pressure of 5.0 MPa. Space velocities from 1000 to 10000 ml·(g cat)$^{-1}$·h^{-1} were used to test the catalytic behavior. At the space velocity of 1000 ml·(g cat)$^{-1}$·h^{-1}, CO_2 conversion was about 0.262. When it was increased to 10000 ml·(g cat)$^{-1}$·h^{-1},

the CO_2 conversion was decreased to 0.232. A decreasing trend was shown in CO_2 conversion and methanol yield. But it was noticed that the CO_2 conversion decrease was 11.4%, while the methanol yield was decreased 31.0% from a space velocity of 1000 ml·(g cat)$^{-1}$·h^{-1} to 10000 ml·(g cat)$^{-1}$·h^{-1}. With a higher space velocity, more reactant was introduced into the reactor and the residence time was shorter, and CO_2 conversion decreased. Here, the reverse water shift reaction was much faster than the methanol synthesis reaction, and the higher space velocity had less effect on the reverse water shift reaction than methanol synthesis, which caused methanol yield to decrease more.

4 KINETICS FOR METHANOL SYNTHESIS FROM CO₂ HYDROGENATION

4.1 Kinetic modeling

Various kinetic models have been proposed for this process. Natta derived a model based on the ZnO/Cr_2O_3 catalyst of the high pressure process, which has now been almost completely abandoned owing to the present favor of the low pressure process [25]. Bakemeier *et al.* noted an important discrepancy between their experimental observations on ZnO/Cr_2O_3 and Natta's kinetics, particularly in the case of CO_2 rich feeds [26]. For this reason, a CO_2 dependency was introduced into the equation using a Langmuir type isotherm. Leonov *et al.* [27] were the first to model methanol synthesis kinetics over a $Cu/ZnO/Al_2O_3$ catalyst. Their model again assumed CO to be the source of carbon in methanol and did not account for the influence of CO_2 in the feed. Klier *et al.* no longer considered CO to be the only carbon source, but still considered it the most important source of carbon in methanol [28]. Villa *et al.* realized that a thorough modeling of the methanol synthesis system should also include a description of the water gas shift reaction [29]. Graaf *et al.* considered both the hydrogenation of CO and CO_2 and the water gas shift reaction [30, 31]. Inspired by the work of Herman *et al.* [32], Graaf *et al.* proposed a dual site mechanism, with CO and CO_2 adsorbing on an s1 type site and H_2 and water adsorbing on a site s₂. The formation of methanol from CO and CO_2 occurs through successive hydrogenations, while the water gas shift reaction proceeds along a formate route. Assuming adsorption and desorption to be in equilibrium and taking every elementary step in each of the three overall reactions in turn as rate determining, Graaf *et al.* examined 48 possible models and used statistical discrimination to get the final set of kinetic equations, which are used below.

In our case, the fibrous Cu/Zn/Al/Zr catalyst showed high activity for producing methanol from CO_2 hydrogenation. Thus, there are three independent reactions present in methanol synthesis from CO_2, namely, Methanol synthesis from CO:

$$CO + 2H_2 = CH_3OH - 90.4 \ kJ·mol^{-1} \quad (6)$$

Reverse water gas shift:

$$CO_2 + H_2 = CO + H_2O + 41.0 \ kJ·mol^{-1} \quad (7)$$

Methanol synthesis from CO_2:

$$CO_2 + 3H_2 = CH_3OH + H_2O - 49.3 \ kJ·mol^{-1} \quad (8)$$
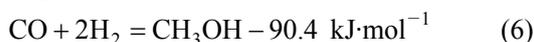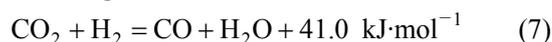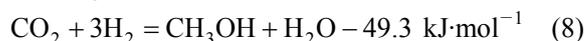
Since the time for reaction (7) to reach thermodynamic equilibrium is very short, it is valid to believe that even for CO_2 hydrogenation, the CO can be converted into CO_2 and adsorb on the Cu site, so the kinetics is the same for CO hydrogenation and CO_2 hydrogenation. Among the above models, Graaf's model [30, 31] gave a better fit and was chosen in our case. The kinetic rate equations for (6)−(8) are as follows:

$$r_1 = \frac{k_1 K_{CO}\left[f_{CO} f_{H_2}^{3/2} - f_{CH_3OH}/\left(f_{H_2}^{1/2} K_{f1}\right)\right]}{\left(1 + K_{CO} f_{CO} + K_{CO_2} f_{CO_2}\right)\left[f_{H_2}^{1/2} + \left(K_{H_2O}/K_{H_2}^{1/2}\right)f_{H_2O}\right]} \quad (9)$$

$$r_2 = \frac{k_2 K_{CO_2}\left(f_{CO_2} f_{H_2} - f_{H_2O} f_{CO}/K_{f2}\right)}{\left(1 + K_{CO} f_{CO} + K_{CO_2} f_{CO_2}\right)\left[f_{H_2}^{1/2} + \left(K_{H_2O}/K_{H_2}^{1/2}\right)f_{H_2O}\right]} \quad (10)$$

$$r_3 = \frac{k_3 K_{CO_2}\left[f_{CO_2} f_{H_2}^{3/2} - f_{CH_3OH} f_{H_2O}/\left(f_{H_2}^{3/2} K_{f3}\right)\right]}{\left(1 + K_{CO} f_{CO} + K_{CO_2} f_{CO_2}\right)\left[f_{H_2}^{1/2} + \left(K_{H_2O}/K_{H_2}^{1/2}\right)f_{H_2O}\right]} \quad (11)$$

where K_{f1}、K_{f2} and K_{f3} are the equilibrium constants of the three reactions, respectively. They were determined by the thermodynamic model proposed by Wang *et al* [33]. K_{CO}, K_{CO_2}, $K_{H_2O}/K_{H_2}^{0.5}$, are the adsorption equilibrium constants of CO, CO_2, H_2O and H_2 [32]. The expressions, $k_i = A_i \exp\left(-E_i/RT\right)$, are the rate constants of each individual reaction. The experimental data as show in Figs. 2−4 are used to fit the kinetic model and the fugacity in Eqs. (9)−(11) was assumed equally to the partial pressure. As we know the reactor size and catalyst amount in the reactor, then the conversion of the CO_2 can be obtained by integration. The parameter estimation was the optimization value of F which was defined as follows:

$$F = \sum_{j=1}^{M}\left[\left(X_{CO_2,exp} - X_{CO_2,cal}\right)^2 + \left(Y_{MeOH,exp} - Y_{MeOH,cal}\right)^2\right] \quad (12)$$

where X and Y was obtained by integration of the reaction rate. The initial value of each parameter was estimated and the simplex method was used as the algorithms to realize the optimization. It was converged
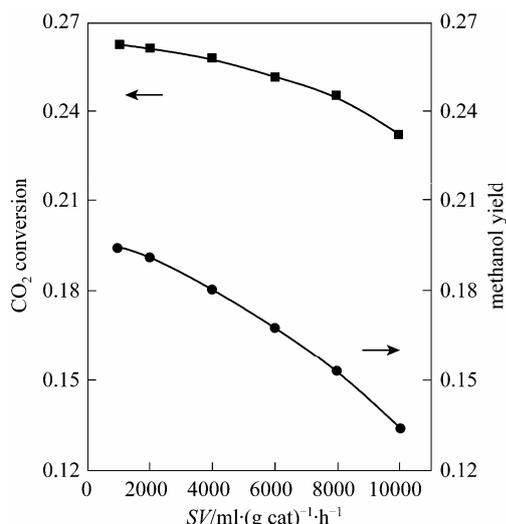
Figure 4 Relationship between the space velocity and CO$_2$ conversion and methanol yield (y_{H_2} : y_{CO_2} = 3 : 1, T = 523 K, p = 5 MPa)

when the residual was less than 10^{-9}. The best fit kinetic parameters are listed in Table 1. Now a model for methanol synthesis on Cu/Zn/Al/Zr catalyst was obtained and it can be used predicted the CO$_2$ conversions and methanol yields. The prediction value can be compared with the experimental results as shown in Fig. 5. The fit is good, with an average deviation of about 5%, and can be predicted the methanol synthesis as follows.
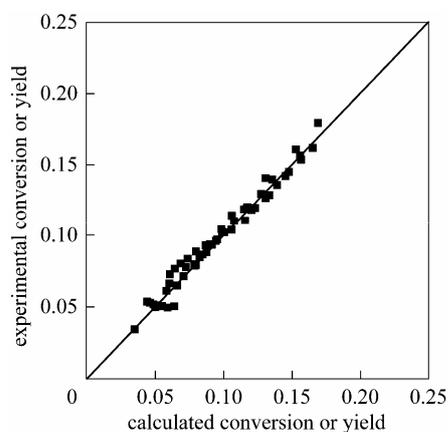
Figure 5 Comparison of model and experimental results

Table1 Regression parameters of the kinetic model

Parameter	A_i	B_i or $-E_i$
K_{CO}	8.3965×10^{-11}	1.1827×10^5
K_{CO_2}	1.7214×10^{-10}	8.1287×10^4
$K_{H_2O} / K_{H_2}^{1/2}$	4.3676×10^{-12}	1.1508×10^5
k_1	4.0638×10^{-6}	-1.1695×10^4
k_2	9.0421×10^8	-1.1286×10^5
k_3	1.5188×10^{-33}	-2.6601×10^5

Note: $K_i = A_i \exp(B_i / RT)$, $k_i = A_i \exp(-E_i / RT)$.

4.2 Simulation of the CO cycle process with the empirical kinetic model

Once the Cu/Zn/Al/Zr catalytic behavior has been quantified, a process, which contains the methanol synthesis in a fixed bed reactor can be simulated with the above kinetic model. When CO was added into the feeding gas, the reactant ratio was changed, and then the reaction rate also changed. This can be predicted using the Graaf's model with the regression parameters. Take an example, 3% CO$_2$ was replaced by CO in the feed gas to the reactor, the calculation result was shown in Fig. 6. It can be seen that both the methanol yield increased. With temperature higher, the increase is more obviously. At 533 K, then the yield of methanol was increase from 0.145 to 0.182 (Fig. 6). With CO addition in the reactant, higher CO$_2$ and H$_2$ concentration can be obtained, then more CO$_2$ and H$_2$ molecular will absorb on the catalyst surface and yield of the methanol increased.
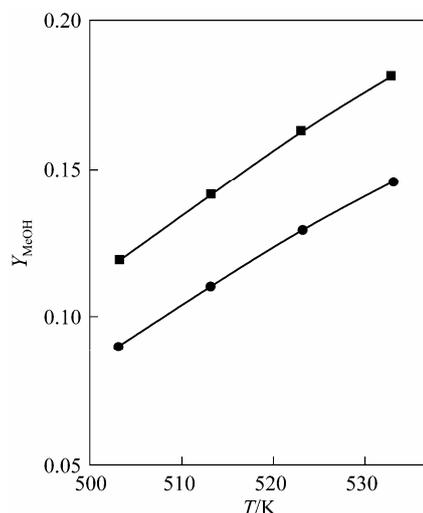
Figure 6 Effect of CO in the methanol synthesis process [y_{H_2} : ($y_{CO} + y_{CO_2}$) = 3 , SV = 6000 ml·(g cat)$^{-1}$·h^{-1}] ■ y_{CO} = 0.03 ; ● y_{CO} = 0

It is noticed that CO is inevitably produced for methanol production in a single reactor. Both CO and CO$_2$ exist in the effluent gas of the reactor. For an industrial process, CO should be separated from the product at first. It even can be fed into the reactor to accelerate the methanol production in the reactor and cycle in the economic process. Thus, a process with CO recycle was design as shown in Fig. 7. The light component, such as CO, unreacted H$_2$, CO$_2$, can be separated in the first distiller and mixed with inlet. The methanol can also obtain at the cooler. The key for the zero CO production process was the highly efficient separation of the effluent gas and delicate control of reactor operation. Those were difficult to realize in our experiment. However, the operation parameters, including the product composition with a fixed value of $(y_{CO} + y_{CO_2})/y_{H_2}$, temperature and
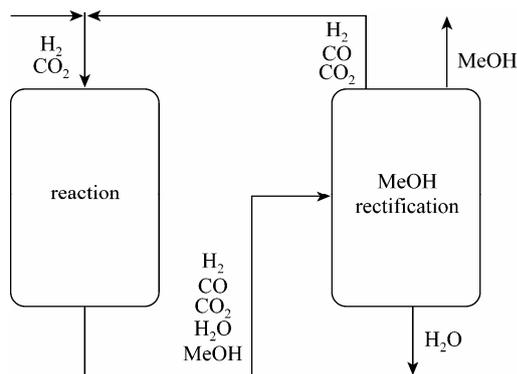
Figure 7 Proposed CO₂ hydrogenation process with CO recycled in the system

pressure, can be obtained by simulation with the present kinetic model for the designated reactor size. For a stable zero CO production in CO_2 hydrogenation, the CO amount that exits the reactor must be equal to the CO amount that enters the reactor. So the stable state can be obtained from the iteration from the design calculation based on the kinetic model. Here, the space velocity was assumed at 6000 ml·(g cat)$^{-1}$·h^{-1}, the ratio of H_2 to CO_2 and CO was 3, the ratio of CO to CO_2 is 3∶22, the reactor size is the same as we used in the Cu/Zn/Al/Zr catalyst evaluation, thus, the operated temperature is related to the pressure. By iterative calculation, the relation between the reaction pressure and temperature can be obtained and was shown in Table 2. When the temperature increased, the related operating pressure also increased. Meanwhile, the space time yield of methanol predicted from the proposed operation is shown in Table 2. Compared with that without recycle, the yield of methanol increased. This was mainly attributed CO acceleration as shown in Fig. 6 and the CO recycle in the methanol synthesis process. From the simulation results, the CO cycle is really important concept for increase the space time yield of methanol in industry process in future.

Table 2 Methanol yield from CO₂ hydrogenation with/without CO recycle and pressures for a stable process with CO recycle at various temperatures

T/K	P/MPa	Space time yield of MeOH/g·(g cat)$^{-1}$·h^{-1}	
		With recycle	Without recycle
503	2.51	0.255	0.193
513	3.07	0.303	0.237
523	3.83	0.350	0.278
533	4.78	0.389	0.313

5 CONCLUSIONS

A fibrous Cu/Zn/Al/Zr catalyst was used to catalyze CO_2 hydrogenation. High CO_2 conversion and methanol yield were obtained at the optimum reaction temperature, high pressure and low space velocity.

The kinetics parameters used were obtained by regression from experimental data. Simulation results showed good agreement with the experimental results. A process for CO_2 hydrogenation with CO recycle is proposed. Base on the simulation, the space time yield of methanol increased and there is no CO in the product stream, which shows good potential application for industry.

NOMENCLATURE

f_i	fugacity of component j, Pa
K_{fi}	equilibrium constant for reaction i
K_j	equilibrium constant for adsorption of component j
M	molecular weight, g·mol^{-1}
p	pressure, MPa
r	reaction speed, mol·(g cat)$^{-1}$·s^{-1}
S	space time yield, g·(g cat)$^{-1}$·h^{-1}
T	temperature, K
V	space time velocity, ml·(g cat)$^{-1}$·h^{-1}
X	conversion
Y	yield

REFERENCES

1 Jean-Paul, L., "Methanol synthesis: a short review of technology improvements", *Catal. Today*, **64**, 3−8 (2001).
2 Hironori, A., "Research and development on new synthetic routes for basic chemicals by catalytic hydrogenation of CO_2 studies", *Surf. Sci. Catal*, **114**, 19−30 (1998).
3 Roman-Martinez, M.C., Cazorla-Amoros, D., Linares-Solano, A., Salinas Martinez, C., "CO₂ hydrogenation under pressure on catalysts Pt-Ca/C", *Appl. Catal. A*, **134**, 159−167 (1996).
4 Takeshi, K., Itaru, H., Hirotaka, M., Kozo, M., Kenji, U., Taiki, W., Masahiro, S., "Kinetic study of methanol synthesis from carbon dioxide and hydrogen", *Appl. Organometal. Chem.*, **15**, 121−126 (2001).
5 Kenji, U., Kozo, M., Takeshi, K., Taiki, W., Masahiro, S., "Methanol synthesis from CO_2 and H_2 in a bench-scale test plant", *Appl. Organometal. Chem.*, **14**, 819−825 (2000).
6 Ortelli, E.E., Wambaca, J., Wokaun A., "Methanol synthesis reactions over a CuZr based catalyst investigated using periodic variations of reactant concentrations", *Appl. Catal. A*, **216**, 227−241 (2001).
7 Melian-Cabrera, I., Granados, M.L., Terreros, P., Fierro, J.L.G., "CO₂ hydrogenation over Pd-modified methanol synthesis catalysts", *Catal. Today*, **45**, 251−256 (1998).
8 Melian-Cabrera, I., Granados, M.L., Fierro, J.L.G., "Effect of Pd on Cu-Zn catalysts for the hydrogenation of CO_2 to methanol: stabilization of Cu metal against CO_2 oxidation", *Catal. Lett.*, **79**, 165−170 (2002).
9 Melian-Cabrera, I., Granados, M.L., Fierro, J.L.G., "Reverse topotactic transformation of a Cu-Zn-Al catalyst during wet Pd impregnation: Relevance for the performance in methanol synthesis from CO_2/H_2 mixtures", *J. Catal.*, **210**, 273−284 (2002).
10 Melian-Cabrera, I., Granados, M.L., Fierro, J.L.G., "Structural reversibility of a ternary CuO-ZnO-Al₂O₃ ex hydrotalcite-containing material during wet Pd impregnation", *Catal. Lett.*, **84**, 153−161 (2002).
11 Cao, Y., Chen, L.F., Dai, W.L., Fan, K.N., Wu, D., Sun, Y.H., "Preparation of high performance Cu/ZnO/Al₂O₃ catalyst for methanol synthesis from CO_2 hydrogenation by coprecipitation-reduction", *Chem. J. Chin. U.*, **24**, 1296−1298 (2003).
12 An, X., Ren, F., Li, J.L., Wang, J.F., "A highly active Cu/ZnO/Al₂O₃ nanofiber catalyst for methanol synthesis through CO_2 and CO hydrogenation", *Chin. J. Catal.*, **26**, 729−730 (2005).
13 Yang, R.Q., Zhang, Y., Noritatsu, T., "Spectroscopic and kinetic analysis of a new low-temperature methanol synthesis reaction", *Catal. Lett.*, **106**, 153−159 (2006).
14 Schuyten, S., Wolf, E.E., "Selective combinatorial studies on Ce and Zr promoted Cu/Zn/Pd catalysts for hydrogen production *via*

methanol oxidative reforming", *Catal. Lett.*, **106**, 7−14 (2006).

15 Zhang, X.R., Wang, L.C., Yao, C.Z., Cao, Y., Dai, W.L., He, H.Y., Fan, K.N., "A highly efficient Cu/ZnO/Al₂O₃ catalyst *via* gel-coprecipitation of oxalate precursors for low-temperature steam reforming of methanol", *Catal. Lett.*, **102**, 183−190 (2005).

16 An, X., Li, J.L., Zuo, Y.Z., Zhang, Q., Wang, D.Z., Wang, J.F., "A Cu/Zn/Al/Zr fibrous catalyst that is an improved CO₂ hydrogenation to methanol catalyst", *Catal. Lett.*, **118**, 264−269 (2007).

17 Sahibzada, M., Metcalfe, I.S., Chadwick, D., "Methanol synthesis from CO/CO₂/H₂ over Cu/ZnO/Al₂O₃ at differential and finite conversions", *J. Catal.*, **174**, 111−118 (1998).

18 Li, F.X., Wang, Y., Wang, D.Z., Wei, F., "Characterization of single-wall carbon nanotubes by N₂ adsorption", *Carbon*, **42**, 2375−2383 (2004).

19 Zhang, Q., Qian, W.Z., Wen, Q., Liu, Y., Wang, D.Z., Wei, F., "The effect of phase separation in Fe/Mg/Al/O catalysts on the synthesis of DWCNTs from methane", *Carbon*, **45**, 1645−1650 (2007).

20 Wang, J.Y., Wang, X.H., Zeng, C.Y., Wu, C.Z., "Intrinsic kinetics of dimethyl ether synthesis directly from CO₂ hydrogeneration", *Acta Petrol Ei Sinica*, **23**, 62−68 (2007). (in Chinese)

21 Chen, L.J., Guo, S.H., Zhao, D.S., "Oxidative desulfurization of simulated gasoline over metal oxide-loaded molecular sieve", *Chin. J. Chem. Eng.*, **15**, 520−523 (2007).

22 An, X., Zuo, Y.Z., Zhang, Q., Wang, D.Z., Wang, J.F., "Dimethyl ether synthesis from CO₂ hydrogenation on a CuO-ZnO-Al₂O₃-ZrO₂/ HZSM-5 bifunctional catalyst", *Ind. Eng. Chem. Res.*, **47**, 6547−6554 (2008).

23 Ma, L., Zhang, Y., Yang, J.C., "Purification of lactic acid by heterogeneous catalytic distillation using ion-exchange resins", *Chin. J. Chem. Eng.*, **13**, 24−31 (2005).

24 An, X., Li, J.L., Wang, J.F., "Thermodynamic analysis for direct synthesis of dimethyl ether from CO and/or CO₂ hydrogenation",

25 Natta, G., In Catalysis, Emmett, P.H., Eds, Reinhold, New York, USA, **3**, 349 (1955).

26 Bakemeier, H., Laurer, P.R., Schroder, W., "Development and application of a mathematical model of the methanol synthesis", *Chem. Eng. Prog. Symp. Ser.*, **66**, 1−10 (1970).

27 Leonov, V.E., Karavaev, M.M., Tsybina, E.N., Petrishcheva, G.S., "Kinetics of methanol synthesis on a low-temperature catalyst", *Kinet. Katal*, **14**, 970−975 (1973).

28 Klier, K., Chatikavanij, V., Herman, R.G., Simmons, G.W., "Catalytic synthesis of methanol from CO/H₂ (IV) the effects of carbon dioxide", *J. Catal.*, **74**, 343−360 (1982).

29 Villa, P., Forzatti, P., Buzzi-Ferraris, G., Garone, G., Pasquon, I., "Synthesis of alcohols from carbon oxides and hydrogen (1) Kinetics of the low-pressure methanol synthesis", *Ind. Eng. Chem. Process. Des. Dev.*, **24**, 12−19 (1985).

30 Graaf, G.H., Stamhuis, E.J., Beenackers, A.A.C.M., "Kinetics of low-pressure methanol synthesis", *Chem. Eng. Sci.*, **43**, 3185−3195 (1988).

31 Graaf, G.H., Scholtens, H., Stamhuis, E.J., Beenackers, A.A.C.M., "Intra-particle diffusion limitations in low-pressure methanol synthesis", *Chem. Eng. Sci.*, **45**, 773−783 (1990).

32 Herman, R.G., Klier, K., Simmons, G.W., Finn, B.P., Bulko, J.B., Kobylinski, T.P., "Catalytic synthesis of methanol from carbon monoxide/hydrogen (I) Phase composition, electronic properties, and activities of the copper/zinc oxide/M₂O₃ catalysts", *J. Catal.*, **56**, 407−429 (1979).

33 Wang, C.W., Ding, B.Q., Zhu, B.C., Luo, Z.C., "Study on phase equilibrium for binary system of gas components, methanol and water in three-phase methanol synthesis process with liquid paraffin", *J. Chem. Eng. Chin. U.*, **14**, 588−592 (2000).

Nat. Gas Chem. Ind., **32**, 5−8 (2007). (in Chinese)